



HAL
open science

Life-history phenology strongly influences population vulnerability to toxicants: a case study with the mudsnail *Potamopyrgus antipodarum*.

Romain Coulaud, Jacques Mouthon, Hervé Quéau, Sandrine Charles, Arnaud Chaumot

► **To cite this version:**

Romain Coulaud, Jacques Mouthon, Hervé Quéau, Sandrine Charles, Arnaud Chaumot. Life-history phenology strongly influences population vulnerability to toxicants: a case study with the mudsnail *Potamopyrgus antipodarum*.. *Environmental Toxicology and Chemistry*, 2013, 32 (8), pp.1727-36. 10.1002/etc.2235 . hal-00972342

HAL Id: hal-00972342

<https://hal.science/hal-00972342v1>

Submitted on 16 May 2020

HAL is a multi-disciplinary open access archive for the deposit and dissemination of scientific research documents, whether they are published or not. The documents may come from teaching and research institutions in France or abroad, or from public or private research centers.

L'archive ouverte pluridisciplinaire **HAL**, est destinée au dépôt et à la diffusion de documents scientifiques de niveau recherche, publiés ou non, émanant des établissements d'enseignement et de recherche français ou étrangers, des laboratoires publics ou privés.

1 *Life-history phenology strongly influences population vulnerability to toxicants: a case*
2 *study with the mudsnail Potamopyrgus antipodarum*

3

4 **Authors:**

5 Romain Coulaud^{§#}, Jacques Mouthon[§], Hervé Quéau[§], Sandrine Charles^{#□}, Arnaud Chaumot^{§£}

6

7 affiliations:

8 [§] Irstea, UR MALY, F-69626 Villeurbanne, France.

9 [#] Université de Lyon, F-69000, Lyon ; Université Lyon 1 ; CNRS, UMR5558, Laboratoire de
10 Biométrie et Biologie Evolutive, F-69622 Villeurbanne, France.

11 [□] Institut Universitaire de France, 103, bd Saint-Michel, 75005 Paris, France.

12 **Abstract**

13 One of the main objectives of ecological risk assessment is to evaluate the effects of
14 toxicants on ecologically relevant biological systems such as populations or communities.
15 However, the effects of toxicants are commonly measured on selected sub-individual or
16 individual endpoints due to their specificity against chemical stressors. Introducing these
17 effects into population models is a promising way to predict impacts on populations. Yet
18 currently employed models are very simplistic and their environmental relevance needs to be
19 improved to establish the ecological relevance of hazard assessment. This study with the
20 gastropod *Potamopyrgus antipodarum* combines a field experimental approach with a
21 modelling framework. It clarifies the role played by seasonal variability of life-history traits in
22 the population's vulnerability to the alteration of individual performance, potentially caused
23 by toxic stress. The study comprised three steps: (i) characterization of the seasonal variability
24 of the life-history traits of a local population over 1 year with *in situ* experiments on caged
25 snails, coupled with a demographic follow-up, (ii) development of a periodic matrix
26 population model which visualizes the monthly variability of population dynamics, and (iii)
27 simulation of the demographic consequences of an alteration of life-history traits (*i.e.*,
28 fertility, juvenile and adult survival). The results revealed that demographic impacts strongly
29 depend on the season when alterations of individual performance occur. Model analysis
30 showed that this seasonal variability of population vulnerability is strongly related to the
31 phenology of the population. We underline that improving the realism of population models is
32 a major objective for ecological risk assessment, and that taking into account species
33 phenology in modelling approaches should be a priority.

34

35 Keywords (limit 5 keywords):

36 Phenology, life-history, *in situ* caging, ecological risk assessment, population modelling

37 **1. Introduction**

38 Biological effects of toxicants are most frequently assessed in terms of alteration of
39 sub-individual or individual performance (*e.g.*, biomarkers) by means of bioassays or field
40 monitoring. Nevertheless, for ecological risk assessment, these impacts on populations,
41 communities and ecosystems are of primary concern [1-8]. Unfortunately, supplying an
42 ecologically relevant assessment by measuring toxic impacts directly on these complex
43 integrated systems is challenging, particularly because distinguishing toxicant impacts from
44 the effects of other environmental factors or anthropogenic stressors can be difficult. One
45 alternative methodology links the effects observed on individual-level endpoints measured in
46 toxicity tests (in the laboratory or during *in situ* experiments) to impacts on populations [9-
47 11]. However, a major problem is the complex relationship between the effects measured at
48 the individual level and outcomes occurring at the population level [12-14]. Introducing the
49 effects of toxicants on demographic parameters (*i.e.*, related to life-history traits) into
50 population models is one way to investigate this relation and to anticipate impacts at the
51 population level [10, 15-16]. In fact, such mechanistic ecological models provide a
52 quantitative way of integrating multiple individual-level endpoints, including survival, growth
53 and reproduction, in projections of population-level consequences such as changes in
54 population abundance or growth rate [17].

55 A large number of studies have demonstrated the value of using demographic models
56 in an ecotoxicological context (reviewed in Galic et al. 2010). However, despite attempts to
57 use more elaborate modelling approaches that integrate environmental complexity [18-23],
58 the ecological relevance of the population models involved is generally low. In fact, in the
59 great majority of studies, demographic models are based on laboratory assays with species
60 that are not representative of the ecosystems of interest (*e.g.* tropical fishes or daphnids for
61 studies on lotic and temperate systems). These models are popular and useful tools for

62 isolating the effects of a toxicant on the population growth rate [7], but they could fail to
63 understand what occurs in the field on local populations [24]. In fact, the determinants of
64 demographic sensitivity of populations are subject to strong variability (*e.g.*, interspecies and
65 interpopulation variability of life cycle). This variability cannot be taken into account with
66 overly simple demographic models [6, 18, 25-26]. Notably, these models do not capture the
67 seasonal variability of population dynamics, even though several studies have underlined a
68 seasonal variability of population vulnerability. A study on the crustacean amphipod
69 *Corophium volutator* [27] showed that the same level of mortality impacts the population
70 differently depending on the season at which mortality occurs. Similarly, in field studies on
71 the amphipod *Leptocheirus plumulosus*, McGee and Spencer [28-29] highlighted a strong
72 monthly variability of the sensitivity of the population growth rate to the different life-history
73 traits. Thus, we need to develop population models which can integrate the seasonal
74 variability of population dynamics to propose a more ecologically relevant assessment of the
75 impact of toxicants on freshwater populations.

76 In the present study, we illustrate the strength of a field experimental approach (*in situ*
77 caging and demographic follow-up) with a modelling framework (periodic matrix model) to
78 decipher the role of seasonality in the vulnerability of populations to toxicants. The model
79 organism is the widespread mudsnail *Potamopyrgus antipodarum* (Gray). We selected this
80 species due to its sensitivity to a large range of chemicals for ecotoxicological tests in the
81 laboratory [30-34] or in the field [35-36]. Notably, *P. antipodarum* is proposed to the
82 Organization for Economic Cooperation and Development (OECD) as a relevant test species
83 to assess the impacts of endocrine disruptors on freshwater molluscs [37]. In the first step we
84 characterized the seasonal variability of the life-history traits of a population of *P.*
85 *antipodarum* over 1 year, with experiments on caged snails and a demographic follow-up of
86 the population. In the second step, we developed periodic matrix population models which

87 allowed us to describe the demographic changes of this population and to picture the monthly
88 variability of its dynamics. In the third step, we simulated the demographic consequences for
89 this population of an alteration of life-history traits (*e.g.*, reduction in fertility, juvenile or
90 adult survival), in order to illustrate the importance of the seasonal variability of population
91 dynamics for ecological risk assessment of chemicals.

92

93 **2. Material and methods**

94 2.1. Biological data

95 *P. antipodarum* is a deposit-feeding gastropod which in Europe reproduces mainly by
96 parthenogenesis of female populations [38]. We conducted a battery of experiments on a
97 population on the Upper Rhône, in the Villebois reservoir (05°27'55.3 E; 45°46'30.7 N,
98 Rhône, France). This site was selected because it contains durable populations of freshwater
99 molluscs monitored for more than one decade [39] and because it was accessible all year
100 round (the water-level fluctuations do not exceed 0.50 m during the year). Temperature was
101 continuously recorded every 2 h using the Tinytag Aquatic 2[®] temperature logger.

102 To characterize the different life-history traits and the population dynamics of *P.*
103 *antipodarum*, we used an *in situ* approach. Firstly, we conducted experiments with snails
104 caged on the study site at different seasons for life-history trait quantification: fertility (*i.e.*,
105 number of neonates produced per reproductive female per day) and growth (*i.e.*, increase of
106 shell length (SL) of juveniles and adults). Secondly, we carried out a demographic follow-up
107 based on a monthly population census to estimate the time-course in population
108 characteristics: densities, SL structure and fecundity (*i.e.*, number of embryos in the brood
109 pouch).

110

111 2.1.1. *In situ* caging experiments

112 *In situ* caging experiments were conducted from October 2009 to November 2010
113 during 10 campaigns lasting 21 days. We measured contrasted environmental conditions
114 between the different campaigns. In this way, mean water temperature, which is known to
115 strongly influence *P. antipodarum* life-history traits [40-43], varied from 4.6 to 22.7 °C. We
116 focused our experiments on measuring fertility and growth. During the year, we were able to
117 study fertility during eight campaigns (insufficient numbers of adults during winter) and
118 growth during seven campaigns (insufficient numbers of juveniles during three campaigns in
119 summer and autumn). Snails were sampled and calibrated (*i.e.*, size selection) directly at the
120 study site. Initial SL was measured each time with a sample of 30 snails. SL was measured
121 between the apex and the distal extremity of the aperture under the binocular microscope,
122 which corresponded to the maximal height of the shell. Initial SL varied from 2.28 (\pm 0.16)
123 mm to 2.85 (\pm 0.34) mm for juveniles and from 4.38 (\pm 0.22) to 4.68 (\pm 0.34) for adults
124 between the different campaigns.

125 Four replicates of 30 juveniles and four replicates of 50 adults were used for growth
126 and fertility measurement. Snails were placed in polypropylene cylindrical containers
127 (diameter, 10 cm; length, 12 cm) with pieces of net (mesh size, 100 μ m) on perforations to
128 allow water flow. Because *P. antipodarum* lives in the upper layers of the sediments [41], a 2-
129 cm layer of sediment removed from the study site and sieved at 315 μ m (*i.e.*, keeping out
130 autochthonous snails) was added to the containers. Two containers with sediment but without
131 snails were deployed for each campaign as control of the absence of autochthonous snails.
132 Finally, containers were placed in a perforated protective case in polyvinylchloride (PVC)
133 with fixing elements for the containers. The containers were placed on the bottom of the river,
134 in close proximity to the site used for the demographic follow-up (see below) at a depth about
135 1.2 m. After the 21-day exposure period, juveniles and adults were fixed with 20% alcohol
136 and measured in the laboratory in order to estimate the snails' daily growth rates. Neonates

137 laid during the period were also fixed with 20% alcohol and counted under a binocular
138 microscope. Then we estimated the fertility rates b (*i.e.*, number of neonates produced by
139 snail per day) as follows:

$$140 \quad b_i = \frac{n_i}{((l_{i,0} + l_{i,t}) / 2) \times t} \quad (1)$$

141 where b_i corresponds to the fertility rate of the replicate i ; n_i to the number of neonates laid in
142 the replicate i ; t is the duration in days of the experiment (here $t = 21$ days for all assays); $l_{i,0}$
143 and $l_{i,t}$ are the number of living snails at the start and at the end of the experiment (here $l_{i,0} =$
144 50 for all assays).

145

146 2.1.2. Demographic follow-up

147 A monthly demographic follow-up was performed from October 2009 to November
148 2010. For each month, snails were sampled in four stations along a 300-m transect at a depth
149 from 0.50 to 1.5 m using a rectangular hand-net (25 × 18 cm); the total area sampled was 1
150 m². Samples were fixed on-site in 20% alcohol. Then we measured the SL of the snails
151 present in a sub-sample corresponding to 9 out of 25 of the total sample in order to estimate
152 monthly population densities and SL distributions. Considering 5% percentiles in SL
153 distribution of juveniles, reproductive individuals and total individuals, we also determined,
154 for each month, SL at birth, SL at maturity and maximum SL to provide guidance in the
155 choice of the model's size classes. To estimate SL at maturity, we dissected 30 individuals
156 covering a large range of sizes, and we counted the number of embryos in the brood pouch
157 (*i.e.*, fecundity) according to the methodology described in Duft et al. [44]. This measurement
158 also allowed us to calculate a relationship between SL and fecundity and to estimate the
159 percentage of reproductive individuals for each adult class defined in the model.

160

161 2.2. Modelling framework and demographic analysis

162

163 2.2.1. Definition of the population model

164 We used a periodic Lefkovitch matrix population model with five size classes [15, 45]
165 to capture the dynamics of the *P. antipodarum* population. Periodic matrix models [46-47] are
166 often used to study cyclical temporal variation (*e.g.*, seasonal or interannual) operated within
167 a single projection interval. The models take the form of periodic matrix products. We used
168 size class models, in contrast to most ecotoxicological studies in which age class (Leslie
169 models) or stage class models are employed [16]. We explain this choice with the following
170 arguments: (*i*) a valid method does not exist to determine the age of snails in field populations
171 for this species, (*ii*) we observed a strong correlation between SL and the life-history traits of
172 *P. antipodarum* (growth rate, maturity, fecundity) and (*iii*) in highly variable environments
173 (*e.g.*, contrasted seasonality), the life-history of individuals in such short-living species
174 strongly depends on their date of birth, which makes age a very weak predictor of biological
175 features. This model thus distinguishes two classes of juveniles (J1 and J2) and three classes
176 of adults (A1, A2 and A3). It integrates the heterogeneity of vital rates (survival, growth and
177 fecundity) between size classes throughout the year.

178 Let $n_i(k)$ be the number of individuals of size class i ($i = 1$ for J1, $i = 2$ for J2, $i = 3$ for
179 A1, $i = 4$ for A2 and $i = 5$ for A3) at the beginning of month k . The five $n_i(k)$ can be gathered
180 in a population vector $\mathbf{n}(k)$. Then we can define 12 monthly matrices \mathbf{M}_k which link up the
181 population vectors $\mathbf{n}(k)$ between months k and $k+1$ as follows:

$$182 \quad \mathbf{n}(k+1) = \mathbf{M}_k \mathbf{n}(k) \quad (2)$$

183 with:

$$\mathbf{M}_k = \begin{bmatrix} s_1(k) \left(1 - \sum_{j>1} g_{1,j}(k)\right) & 0 & f_3(k) \sqrt{s_1(k)} \sqrt{s_3(k)} & f_4(k) \sqrt{s_1(k)} \sqrt{s_4(k)} & f_5(k) \sqrt{s_1(k)} \sqrt{s_5(k)} \\ s_1(k) g_{1,2}(k) & s_2(k) \left(1 - \sum_{j>2} g_{2,j}(k)\right) & 0 & 0 & 0 \\ s_1(k) g_{1,3}(k) & s_2(k) g_{2,3}(k) & s_3(k) \left(1 - \sum_{j>3} g_{3,j}(k)\right) & 0 & 0 \\ s_1(k) g_{1,4}(k) & s_2(k) g_{2,4}(k) & s_3(k) g_{3,4}(k) & s_4(k) (1 - g_{4,5}(k)) & 0 \\ s_1(k) g_{1,5}(k) & s_2(k) g_{2,5}(k) & s_3(k) g_{3,5}(k) & s_4(k) g_{4,5}(k) & s_5(k) \end{bmatrix} \quad (3)$$

185 where $s_i(k)$ is the survival rate of the size class i during month k , $g_{i,j}(k)$ the transition rate
 186 between the size classes i and j during month k , and $f_i(k)$ the reproductive rate of the size
 187 class i during month k . The product of the 12 monthly matrices \mathbf{M}_k leads to an annual
 188 periodic matrix \mathbf{L} , which links the population vector from year t to year $t+1$ as follows:

$$\mathbf{n}(t+1) = \left(\prod_{k=1}^{12} \mathbf{M}_k \right) \mathbf{n}(t) = \mathbf{L} \mathbf{n}(t) \quad (4)$$

190 To assess the seasonal variability of the demographic sensitivity of the population, we also
 191 defined four seasonal periodic matrices: \mathbf{L}_A for autumn, \mathbf{L}_W for winter, \mathbf{L}_{SP} for spring and
 192 \mathbf{L}_{SU} for summer. These matrices correspond to the product of the three monthly matrices \mathbf{M}_k
 193 corresponding to each season (*i.e.*, September, October and November in autumn; December,
 194 January and February in winter; March, April and May in spring; and June, July and August
 195 in summer).

196

197 2.2.2. Parameter estimation

198 We estimated the reproductive rates $f_i(k)$ for the three size classes of adults ($i = 3, 4$
 199 and 5) as follows:

$$f_i(k) = b_i(k) \rho_i(k) \Delta t(k) \quad (5)$$

201 where $b_i(k)$ corresponds to fertility (*i.e.*, number of neonates produced by reproductive female
 202 per day) for class i during month k , $\rho_i(k)$ to the percentage of females in reproduction in class
 203 i during month k , and $\Delta t(k)$ to the number of days of month k . $\rho_i(k)$ was estimated with data

204 from the demographic follow-up (see above), and $b_i(k)$ was predicted with the mean monthly
205 water temperature, according to the relationship between mean temperature and fertility
206 established from outcomes of caging experiments. Because only one size class of adults was
207 used for *in situ* caging, we controlled the size effect between classes in the calculation of $b_i(k)$
208 using the relationship between SL and fecundity (*i.e.*, number of embryos in the brood
209 pouch), which is established from the demographic follow-up. Similarly, we calculated the
210 transition rates $g_{i,j}(k)$ using the relationship between growth and temperature estimated in *in*
211 *situ* caging experiments. Using the mean water temperature recorded during month k , we
212 predicted the growth of individuals with size at the limits of each class i between months k
213 and $k+1$, and then we estimated for each size class the proportion of individuals which stayed
214 in size class i , or which attained the larger size classes.

215 It is not possible to estimate the survival rates directly from field experiments. In fact,
216 mark and recapture methodologies, which are currently used for larger organisms (*e.g.*, fish,
217 mammals) are not easy to set up for *P. antipodarum* due to the difficulty marking the snails
218 durably. Alternatively, the survival rates observed with the caged snails were not ecologically
219 relevant (*e.g.*, lack of predation, competition). Therefore, to estimate the survival rates of
220 individuals for a month k , we compared the densities observed during the demographic
221 follow-up in month k to the theoretical densities predicted by the observed densities of month
222 $k-1$ and the growth and reproductive rates of the individuals estimated for month $k-1$.

223

224 2.2.3. Model outcomes, elasticity analyses and simulations

225 The Lefkovich matrix \mathbf{L} is a primitive matrix and can be processed analytically as a
226 Leslie matrix. It presents a first dominant eigenvalue λ , corresponding to the asymptotic
227 population growth rate [15 , 48]. The right eigenvector w associated with this first eigenvalue
228 gives the asymptotic stable size structure. According to the first matrix used in the matricial

229 product of the 12 monthly matrices \mathbf{M}_k , we can obtain the different SL structures at the end
230 of each month of the year. The demographic elasticities were analyzed by simulation with the
231 application of 10% reduction in each life-history trait successively (*i.e.*, survival of each class,
232 fertility and growth) in order to estimate the subsequent relative reduction in the asymptotic
233 population growth rate λ . To examine the between-season variability of population
234 vulnerability, we also simulated the demographic consequences of different levels of
235 alteration of life-history traits at different dates in the year. To accomplish this, reductions
236 from 0% to 100% on fertility, juvenile survival and adult survival were applied to the three
237 months corresponding to each season.

238

239 2.3. Statistical analyses

240 Statistical procedures and population models were all implemented with the R
241 software [49]. Before using parametric analysis (ANOVA procedure), normality and
242 homoscedasticity were checked using the Shapiro-Wilk test and the Bartlett test, respectively.
243 To quantify growth of *P. antipodarum* snails in *in situ* caging, we fitted, independently for
244 each caging experiment, a logistic model on SL data using the *nls* function, simultaneously
245 considering the two categories of caged snails (juveniles and adults) as follows:

$$246 \quad L(t) = \frac{Lmax}{1 + \left(\frac{Lmax}{Linit} - 1 \right) e^{(-r t)}} \quad (6)$$

247 where $L(t)$ corresponds to the SL of snails at time t , $Lmax$ to the maximal SL of snails
248 observed in the population, $Linit$ to the SL of the two categories of caged snails at the
249 beginning of the experiment, r to the daily growth coefficient of the logistic model, and t to
250 the time. We fixed $Lmax$ at 5.5 mm (maximum value observed during the demographic
251 follow-up). No replicate effect was considered when fitting the logistic models (one per
252 campaign), since no significant difference in SL of juveniles and adults were detected

253 between replicates at the end of the test for each one of the seven campaigns. Concerning the
254 seasonal variability of fertility and daily growth, we fitted Gaussian relationships between
255 these life-history traits and water temperature using the *nls* function. For the demographic
256 follow-up, the influences of SL and month on fecundity were tested using linear modelling
257 including the interaction terms (ANOVA procedure).

258

259 3. Results

260

261 3.1. Seasonal variability of life-history traits

262 By means of *in situ* caging experiments, we recorded strong seasonal variability in the
263 production of *P. antipodarum* neonates, which varied from 0 to 0.8 neonates per female per
264 day. This seasonal variability in fertility was highly correlated with water temperature (Figure
265 3A). Thus, we fitted a Gaussian curve to describe fertility b_i (production of neonates per day
266 per reproductive female) as a function of mean water temperature θ (in °C) as follows:

$$267 \quad b_i(\theta) = 6.92 \times e^{\left(\frac{17.91 - \theta}{3.85}\right)^2} \quad (7)$$

268 Fertility is optimal at a temperature of 17.91 °C. Concerning growth, here again we detected
269 strong seasonal variability of individual SL gains, in relation with the mean water temperature
270 (Figure 3B). We used nonlinear regression to fit a Gaussian relationship between growth
271 coefficient r and mean water temperature θ (in °C) as follows:

$$272 \quad r(\theta) = 0.006 + 0.21 \times e^{\left(\frac{18.61 - \theta}{3.72}\right)^2} \quad (8)$$

273 In comparison with fertility, we added a constant parameter in order to take into account a
274 minimal daily growth rate different from 0. In fact, contrary to fertility, which was null during

275 the caging with the lower temperature (Figure 3A), we observed that individuals grow even at
276 low temperatures (Figure 3B). Growth is optimal at 18.61 °C.

277 Concerning the monthly demographic follow-up, the evolution of the population's SL
278 structure is presented in Figure 1. The highest densities were observed in autumn (*e.g.*, more
279 than 10,000 individuals per square metre in October and November) and the lowest in spring.
280 Juveniles (*i.e.*, SL < 3.5 mm, size classes J1 and J2 of the model) are present throughout the
281 year and account for the major part of the population, while adult densities (*i.e.*, SL > 3.5 mm,
282 size classes A1, A2 and A3) show highly variable frequencies during the year. In fact, in
283 winter and spring, the population comprises mainly juveniles, while in summer and autumn
284 adults appear in the population. We estimated a SL at birth of 0.5 (0.1) mm, a SL at maturity
285 of 3.5 (0.2) mm and a maximum SL of 5.2 (0.3) mm. According to these very weak standard
286 deviations, we did not consider monthly differences in the SL at birth, at maturity and the
287 maximum SL for the parameterisation of the population model. Concerning the percentage of
288 individuals in reproduction (*i.e.*, females bearing embryos) $\rho_i(k)$, for all dates of the year,
289 more than 90% of the individuals with a SL greater than 4.2 mm were reproductive.
290 Individuals between 3.5 and 4.2 mm presented a seasonal variability: 50% of individuals were
291 reproductive between November and May and 80% between June and October. We observe a
292 strong positive relationship between SL and fecundity (Figure 2), with no seasonal effect
293 (ANOVA test: interaction terms, $p > 0.1$; seasonal effect, $p > 0.81$; SL effect, $p < 10^{-15}$). In
294 this way, we note that females of the model's A1 size class have a mean fecundity of 12.2
295 embryos; size class A2 females a mean fecundity of 24.3 embryos and size class A3 females a
296 mean fecundity of 37.6 embryos.

297

298 3.2. Population model analysis

299 Regarding parameter estimation, we report a strong between-class and between-month
300 variability of the reproductive rates $f_i(k)$. Between November and March, reproductive rates
301 were very low for all classes due to low water temperatures, while all size classes reproduced
302 between April and October. Depending on the size class and the month, reproductive rates
303 varied from 0.01 to 35.05 neonates per month per individual. Regarding the transition rates
304 $g_{i,j}(k)$, the majority of individuals stayed in their initial size class from month to month
305 during winter and spring, in contrast to summer and autumn, where growth was faster and a
306 great majority of individuals changed one or two size classes over 2 months. Adult survival
307 showed high monthly variability with very low survival rates between January and May and
308 higher survival rates in summer and autumn. Juvenile survival (for size classes J1 and J2) was
309 generally higher than adult survival, particularly in winter and spring. For some months, we
310 calculated survival rates higher than 1, in particular when densities of individuals were low
311 (uncertainty increased with small size samples). For the parameterization of the matrix model,
312 we tested two possibilities: (i) we applied the survival rates keeping the values higher than 1
313 (apparent survivals), or alternatively (ii) we fixed a ceiling level of 1 for maximum survival
314 rates. Despite differences in the absolute value of the asymptotic population growth rate λ , the
315 stable size distribution and elasticity pattern were very similar in both cases. For the following
316 results on model analysis, we chose to use survival rates capped at 1, but conclusions on the
317 demographic behaviour of the population remain unchanged with apparent survival rates.

318 In a first time, we calculated the asymptotic population growth rate λ with the annual
319 periodic matrix L . We found a value of $\lambda = 1.17$. We also computed the stable size
320 distribution for the different seasons that we compared to the population structure observed
321 during the demographic follow-up (Figure 4). We noted good coherence between the model
322 and the field data. Thus, it appears that our mechanistic modelling framework can identify the
323 dynamics of the *P. antipodarum* population throughout the year. In a second time, we

324 characterized the seasonal variability of the demographic fitness of the population by
325 calculating the asymptotic population growth rate of the four periodic seasonal matrices (L_A ,
326 L_W , L_{SP} and L_{SU}). We found 3-month λ values equal to 1.02 in autumn, 0.17 in winter, 0.16
327 in spring and 2.31 in summer. For comparison to the annual matrix L , the standardization of
328 λ to a 3-month time step supplies a value of 1.04. Thus, we underline a strong seasonal
329 variability of snail population dynamics, with a potential growth of the population mainly in
330 summer and autumn.

331 The elasticity analysis on the annual matrix L showed that the asymptotic population
332 growth rate λ was more sensitive to relative changes in juvenile survival (S1 and S2) than to
333 changes in the other life-history traits (Figure 5). The life-history trait corresponding to the
334 second highest elasticity was adult survival (cumulative elasticities of S3, S4 and S5)
335 followed by fertility. Concerning growth (Figure 5), we observe that the population growth
336 rate was not sensitive to relative changes in this life-history trait. On the contrary, we note that
337 a reduction of the daily growth rates strikingly increases the asymptotic population growth
338 rate λ . We also performed elasticity analysis on the four seasonal matrices (L_A , L_W , L_{SP} and
339 L_{SU}) (Figure 6). These analyses reveal two contrasted patterns. On one hand, in spring and
340 winter, the population growth rate was very sensitive to juvenile survival alteration but
341 remained unchanged by reduction in adult survival or reproduction rates. Concerning growth,
342 we observe, as for the annual model, that the reduction of this life-history trait increased the
343 asymptotic population growth rate. On the other hand, in summer and autumn, the population
344 growth rate was sensitive to changes in juvenile survival but also to changes in adult survival,
345 fertility and growth.

346 Strong variability of population impacts (percentage of reduction of the population
347 growth rate λ) can be seen when alterations of life-history traits at different seasons were
348 integrated into the model (Figure 7). In fact, except for juvenile survival for which we noted

349 that the population growth rate was highly affected for all seasons, concerning reproduction
350 and adult survival, between-season differences were substantial. Indeed, the population was
351 very sensitive to impacts on fertility in summer and particularly in autumn, but showed very
352 low sensitivity in spring and winter, even for substantial fertility inhibitions. Furthermore, the
353 population was very sensitive to impacts on adult survival in summer, even for very small
354 inhibitions, but quite insensitive in the other seasons even for considerable inhibitions.

355

356 **4. Discussion**

357

358 4.1. Seasonal variability of life-history traits of *P. antipodarum*

359 We observed fluctuating densities during the year. The high-density pattern at the end
360 of summer and autumn and the low-density pattern in winter and spring agree with previous
361 data obtained during demographic follow-up conducted for *P. antipodarum* [41, 50].
362 Furthermore, these density variations during the year are consistent with the observations of a
363 long-term follow-up of mollusc populations conducted in this study site (data not published
364 for *P. antipodarum*). However, Schreiber et al. [51] observed the highest densities in spring
365 and summer. This contrast with the present study can be explained by the delaying effect of
366 temperature rise due to a large snow-melt upstream of the Rhône watershed. For Richards and
367 Shin [52], these fluctuating densities are driven by density-dependent processes. Nevertheless,
368 in populations with small temperature fluctuations, Quinn et al. [53] observed that densities
369 are very stable during the year, and it is widely accepted that *P. antipodarum* population
370 densities are generally strongly correlated with water temperature [50], consistent with our
371 observations. The population in our case was primarily composed of juveniles, particularly in
372 winter and spring, which agrees with previous data [51, 54]. In this way, the persistence of the
373 population in winter is ensured by the survival of a reserve of juveniles. In summer and

374 autumn, the population is composed of two cohorts, one with small juveniles and one with
375 large adults. The size at birth, size at maturity and maximum size values are consistent with
376 previous reports for this species [30, 51, 54-57]. Similar to Schreiber et al. [51], who observed
377 65% reproductive females in their population, we observed that the majority of females
378 carried embryos. During dissections, we never observed males, as in other studies which
379 stated that the vast majority of European populations of *P. antipodarum* are made up of
380 parthenogenetic females [38] with a few exceptional males [58]. This explains why we did
381 not integrate the sex ratio into our model.

382 The methodology of *in situ* caging implemented here throughout the year provides a
383 useful tool to estimate life-history traits in the field (*e.g.*, realistic exposure conditions, good
384 reproducibility of the assays) [59-60]. Until now, only a few studies have conducted *in situ*
385 experiments with *P. antipodarum* [35-36, 61]. Here, we chose this methodology rather than a
386 laboratory approach in order to obtain environmentally relevant data for the calibration of the
387 population model. In fact, several factors are difficult to control in laboratory conditions, in
388 particular the diet of *P. antipodarum*. Here, we report a strong seasonal variability in neonate
389 production and growth rates. Several studies have shown that *P. antipodarum* life-history
390 traits are strongly correlated with water temperature [40, 42]. The quality of the fits observed
391 in Figure 3 confirms this pattern. The maximum fertility value (0.80 juveniles per day
392 recorded during caging at a mean temperature of 17.5 °C) is higher than the values reported in
393 other studies for this temperature range [30-31]. Nevertheless, all the studies which measured
394 fertility directly (*i.e.*, counting production of neonates) were conducted during laboratory
395 experiments, which probably do not offer optimal conditions for the reproduction of this
396 species. To our knowledge, our study reports for the first time a direct *in situ* measurement of
397 fertility. In fact, in *in situ* assays, fertility is usually estimated indirectly from fecundity (*i.e.*,
398 counting of the number of embryos in the brood pouch) [35-36, 61]. This measure can

399 provide useful information but it remains difficult to predict the realized reproduction of
400 individuals without information on laying dynamics. We estimated an optimal temperature of
401 17.9 °C for fertility. This value is consistent with previous laboratory studies [40, 42]. Schmitt
402 et al. [36] did not observe a relationship between temperature and fertility during different *in*
403 *situ* experiments, but the temperature range was very narrow compared to our experiments.
404 Concerning growth, we estimated an optimal value of 18.7 °C close to the fertility value.
405 Thus, water temperature between 17 and 19 °C appeared to provide optimal conditions for the
406 development of *P. antipodarum*.

407

408 4.2. Demographic insights from the population model analysis

409 The adequacy of the stable size distribution computed for each season with the
410 population size structure observed during the demographic follow-up (Figure 4) illustrates
411 that our modelling framework is able to reliably describe the dynamics of this *P. antipodarum*
412 population taking into account its particular phenology. The analysis of seasonal matrices
413 (\mathbf{L}_A , \mathbf{L}_W , \mathbf{L}_{SP} and \mathbf{L}_{SU}), which simulate population dynamics under hypothetical scenarios of
414 eternal autumn, winter, spring or summer, allows us to underline substantial seasonal
415 variability in the demographic fitness of the population (quantified by the asymptotic growth
416 rate λ). On one hand, winter and spring are seasons with a potential population decrease, and
417 on the other hand, summer and autumn seasons have a high potential for a population
418 increase. This is explained by reproductive rates that are nearly zero in spring and winter
419 along with very low survival rates, in particular for adults.

420 With the annual model, we observed that the population dynamics is particularly
421 sensitive to changes in juvenile survival (Figure 5). This is consistent with the conclusions of
422 several demographic studies on *P. antipodarum* [30, 34, 62]. Pedersen et al. [30], when
423 studying the effects of the polycyclic musk HHCb on individual and population-level

424 endpoints, observed that the asymptotic population growth rate of *P. antipodarum* is
425 approximately four times more sensitive to juvenile survival alteration than to adult survival,
426 and ten times more sensitive to juvenile survival alteration than to fertility inhibition.
427 Surprisingly, we noted that a reduction of the daily growth rate increased the asymptotic
428 population growth rate λ . This unexpected demographic outcome can be explained by the very
429 low survival rates of the last classes of adults for several months in spring and winter. Thus,
430 when the daily growth rate is decreased, individuals stay for more months in the first class of
431 adults with higher survival rates, which increases their cumulative reproductive value for the
432 population. This advantage for organisms with a low growth rate is similar to observations on
433 fish populations under fishing pressure, in which higher mortality rates lead to the selection of
434 individuals with lower growth ability [63-64]. With the seasonal models, we show an
435 important seasonal variability of the pattern of elasticities (Figure 6). In fact, in the same
436 manner as for the population dynamics, we can identify two contrasted periods. In spring and
437 winter, the population is mostly sensitive to the reduction in juvenile survival, while in
438 summer and autumn, the demographic sensitivity to juvenile survival reduction is
439 considerably reduced, and the population demography becomes more sensitive to the
440 alteration of other traits. This strong seasonal variability of population sensitivity is explained
441 by the phenology of the population: in winter and spring, maintenance of the population is
442 ensured by a stock of juveniles (no reproduction, high adult mortality), whereas in summer
443 and autumn, juveniles grow up, mature as adults, and therefore reproduce. Seasonal
444 variability of population sensitivity is also observed in the amphipod *Leptocheirus plumulosus*
445 using a field-based periodic matrix population model [28-29]. Thus, analyzing the elasticity of
446 periodic matrix models can provide valuable insights into the relative importance of the
447 demographic rates at different periods of year.

448

449 4.3. Seasonal variability and field-based population models in ecological risk assessment

450 Despite the substantial seasonal variability of population demographic sensitivity, to
451 our knowledge, only a few ecotoxicological studies have addressed the temporal variability of
452 effects on population dynamics [27-29]. We roughly simulated reductions in fertility, juvenile
453 survival and adult survival at different seasons. Population impacts strongly depend on the
454 season at which toxic effects on individual performance occur (Figure 7). For instance, a time
455 window of high population vulnerability to reproductive alteration is focused in summer and
456 autumn, in contrast to winter and spring, for juvenile mortality. Thus, the development of
457 population models that integrate seasonality is a relevant way to increase our ability to project
458 toxic effects on individual performance into population demographic impacts. As an
459 illustration, when studying HHCB effects on *P. antipodarum*, Pedersen et al. [30] observed
460 significant effects on offspring production up to 42% reduction) but stated that such
461 inhibitions will not give rise to significant impacts on population dynamics. In spring and
462 winter, our simulations agree with this conclusion. However, in summer and particularly in
463 autumn, we anticipate considerable population consequences of such levels of fertility
464 inhibition. In fact, in autumn, we observed that a 40% reduction in fertility means a 30%
465 decrease of the asymptotic population growth rate (Figure 7). Similar to the great majority of
466 studies addressing population extrapolation, the life cycle is roughly parameterized from
467 laboratory data. In fact, life-history traits are often estimated in the controls of the
468 experiments and are not representative of life-history of local populations. Thus, with this
469 laboratory approach, models do not provide valuable information about potential
470 demographic consequences of toxicant impacts in field populations [30]. Laboratory
471 conditions are too favourable (*e.g.*, no predation or competition, water temperature is
472 constant) or in contrast, they fail to provide optimal conditions or complexity for all abiotic
473 and biotic parameters (*e.g.*, oxygenation, water flow, temperature, food, crowding effect). One

474 way currently used to address such concerns about the ecological relevance of population
475 extrapolation consists in exploring a range of values of life-history traits and showing that
476 changes in the population growth rate are low. By this means, authors aim to assess the
477 robustness of their conclusions against divergence in life histories between laboratory and
478 wild populations. For example, Pedersen et al. [30] validated the robustness of their
479 population model by testing three scenarios: decrease in juvenile survival, decrease in
480 juvenile and adult survival, and decrease in juvenile survival, adult survival and fertility. But
481 the range of tested fluctuations is not at all “field-realistic” regarding our field observations:
482 (i) only 50% for fertility, whereas we showed in the *P. antipodarum* population that fertility is
483 very low during a great part of the year with greater reduction than in this study; and (ii) only
484 a 20% reduction in adult survival and a 90% reduction in juvenile survival, while we observed
485 that juvenile mortality is generally lower than adult mortality in the field. Thus, it appears that
486 a field-based approach can be of great interest to guarantee the relevance of hazard
487 assessment at the population level, and to provide realistic scenarios for exploring its
488 soundness with respect to between-population variability of life-histories.

489 Improving the ecological realism of population models is a major concern for
490 ecological risk assessment. Incorporating species phenologies is feasible with modelling
491 approaches and should be one priority when seeking to put the “eco into ecotoxicology” [2].

492

493 **Acknowledgments**

494

495 The authors thank the Cluster Environnement of the Région Rhône-Alpes (France) for
496 financial grants.

497 **References**

498

499 [1] Barnthouse LW, Munns WR, Sorensen MT. 2008. *Population-level ecological risk*
500 *assessment*. SETAC.

501 [2] Chapman PM. 2002. Integrating toxicology and ecology: Putting the 'eco' into
502 ecotoxicology. *Marine Pollution Bulletin* 44:7-15.

503 [3] Forbes VE, Calow P, Grimm V, Hayashi TI, Jager T, Katholm A, Palmqvist A,
504 Pastorok R, Salvito D, Sibly R, Spromberg J, Stark J, Stillman RA. 2011. Adding value to
505 ecological risk assessment with population modeling. *Human and Ecological Risk Assessment*
506 17:287-299.

507 [4] Forbes VE, Calow P, Grimm V, Hayashi T, Jager T, Palmqvist A, Pastorok R,
508 Salvitoy D, Sibly R, Spromberg J, Stark J, Stillman RA. 2010. Integrating population
509 modeling into ecological risk assessment. *Integrated Environmental Assessment and*
510 *Management* 6:191-193.

511 [5] Forbes VE, Palmqvist A, Bach L. 2006. The use and misuse of biomarkers in
512 ecotoxicology. *Environmental Toxicology and Chemistry* 25:272-280.

513 [6] Landis WG. 2006. Population-scale assessment endpoints in ecological risk
514 assessment. Part I: Reflections of stakeholder values. *Integrated Environmental Assessment*
515 *and Management* 2:86-91.

- 516 [7] Raimondo S, McKenney Jr CL. 2006. From organisms to populations: Modeling
517 aquatic toxicity data across two levels of biological organization. *Environmental Toxicology*
518 *and Chemistry* 25:589-596.
- 519 [8] Thorbek P, Forbes VE, Heimbach F. 2009. *Ecological Models for Regulatory Risk*
520 *Assessments of Pesticides: Developing a Strategy for the Future*. CRC Press.
- 521 [9] Levin L, Caswell H, Bridges T, Dibacco C, Cabrera D, Plaia G. 1996. Demographic
522 responses of estuarine polychaetes to pollutants: life table response experiments. *Ecological*
523 *Applications* 6:1295-1313.
- 524 [10] Forbes VE, Calow P. 2002. Extrapolation in Ecological Risk Assessment: Balancing
525 Pragmatism and Precaution in Chemical Controls Legislation. *BioScience* 52:249-257.
- 526 [11] Forbes VE, Calow P, Sibly RM. 2008. The extrapolation problem and how population
527 modeling can help. *Environmental Toxicology and Chemistry* 27:1987-1994.
- 528 [12] Widarto TH, Krogh PH, Forbes VE. 2007. Nonylphenol stimulates fecundity but not
529 population growth rate of *Folsomia candida*. *Ecotoxicology and Environmental Safety* 67:369-
530 377.
- 531 [13] Kammenga JE, Busschers M, Van Straalen NM, Jepson PC, Bakker J. 1996. Stress
532 induced fitness reduction is not determined by the most sensitive life-cycle trait. *Functional*
533 *Ecology* 10:106-111.

534 [14] Stark JD, Banks JE, Vargas R. 2004. How risky is risk assessment: The role that life
535 history strategies play in susceptibility of species to stress. *Proceedings of the National*
536 *Academy of Sciences of the United States of America* 101:732-736.

537 [15] Caswell H. 2001. *Matrix Population Models*. John Wiley & Sons, Ltd.

538 [16] Galic N, Hommen U, Baveco JM, Van Den Brink PJ. 2010. Potential application of
539 population models in the european ecological risk assessment of chemicals II: Review of
540 models and their potential to address environmental protection aims. *Integrated*
541 *Environmental Assessment and Management* 6:338-360.

542 [17] Hanson N. 2011. Population Modeling of the Fish Species Roach (*Rutilus rutilus*) to
543 Investigate How Latitudinal Variations in Life History Traits Affect the Sensitivity to
544 Anthropogenic Stress. *Environmental Modeling and Assessment*:1-11.

545 [18] Ares J. 2003. Time and space issues in ecotoxicology: Population models, landscape
546 pattern analysis, and long-range environmental chemistry. *Environmental Toxicology and*
547 *Chemistry* 22:945-957.

548 [19] Chaumot A, Charles S, Flammarion P, Auger P. 2003. Do migratory or demographic
549 disruptions rule the population impact of pollution in spatial networks? *Theoretical*
550 *Population Biology* 64:473-480.

551 [20] Chaumot A, Charles S, Flammarion P, Auger P. 2003. Ecotoxicology and spatial
552 modeling in population dynamics: An illustration with brown trout. *Environmental*
553 *Toxicology and Chemistry* 22:958-969.

554 [21] Emlen JM, Duda JJ, Kirchhoff MD, Freeman DC. 2006. Interaction Assessment: A
555 modeling tool for predicting population dynamics from field data. *Ecological Modelling*
556 192:557-570.

557 [22] Galic N, Baveco H, Hengeveld GM, Thorbek P, Bruns E, Van Den Brink PJ. 2012.
558 Simulating population recovery of an aquatic isopod: Effects of timing of stress and landscape
559 structure. *Environmental Pollution* 163:91-99.

560 [23] Van Den Brink PJ, Baveco JM, Verboom J, Heimbach F. 2007. An individual-based
561 approach to model spatial population dynamics of invertebrates in aquatic ecosystems after
562 pesticide contamination. *Environmental Toxicology and Chemistry* 26:2226-2236.

563 [24] Hansen F, Forbes VE, Forbes TL. 1999. Using elasticity analysis of demographic
564 models to link toxicant effects on individuals to the population level: an example. *Functional*
565 *Ecology* 13:157-162.

566 [25] Hanson N. 2009. Population level effects of reduced fecundity in the fish species
567 perch (*Perca fluviatilis*) and the implications for environmental monitoring. *Ecological*
568 *Modelling* 220:2051-2059.

569 [26] Hanson N, Stark JD. 2011. A comparison of simple and complex population models to
570 reduce uncertainty in ecological risk assessments of chemicals: example with three species of
571 *Daphnia*. *Ecotoxicology*:1-9.

572 [27] Smit MGD, Kater BJ, Jak RG, van den Heuvel-Greve MJ. 2006. Translating bioassay
573 results to field population responses using a Leslie-matrix model for the marine amphipod
574 *Corophium volutator*. *Ecological Modelling* 196:515-526.

575 [28] McGee BL, Spencer M. 2001. A field-based population model for the sediment
576 toxicity test organism *Leptocheirus plumulosus*: II. Model application. *Marine Environmental*
577 *Research* 51:347-363.

578 [29] Spencer M, McGee BL. 2001. A field-based population model for the sediment
579 toxicity test organism *Leptocheirus plumulosus*: I. Model development. *Marine*
580 *Environmental Research* 51:327-345.

581 [30] Pedersen S, Selck H, Salvito D, Forbes V. 2009. Effects of the polycyclic musk
582 HHCB on individual- and population-level endpoints in *Potamopyrgus antipodarum*.
583 *Ecotoxicology and Environmental Safety* 72:1190-1199.

584 [31] Gust M, Buronfosse T, Giamberini L, Ramil M, Mons R, Garric J. 2009. Effects of
585 fluoxetine on the reproduction of two prosobranch mollusks: *Potamopyrgus antipodarum* and
586 *Valvata piscinalis*. *Environmental Pollution* 157:423-429.

587 [32] Gust M, Garric J, Giamberini L, Mons R, Abbaci K, Garnier F, Buronfosse T. 2010.
588 Sensitivity of New Zealand mudsnail *Potamopyrgus antipodarum* (Gray) to a specific
589 aromatase inhibitor. *Chemosphere* 79:47-53.

- 590 [33] Forbes VE, Moller V, Depledge MH. 1995. *Intrapopulation variability in sublethal*
591 *response to heavy metal stress in sexual and asexual gastropod populations*. Wiley-
592 Blackwell, Oxford.
- 593 [34] Møller V, Forbes VE, Depledge MH. 1996. Population responses to acute and chronic
594 cadmium exposure in sexual and asexual estuarine gastropods. *Ecotoxicology* 5:313-326.
- 595 [35] Gust M, Buronfosse T, Geffard O, Mons R, Queau H, Mouthon J, Garric J. 2010. In
596 situ biomonitoring of freshwater quality using the New Zealand mudsnail *Potamopyrgus*
597 *antipodarum* (Gray) exposed to waste water treatment plant (WWTP) effluent discharges.
598 *Water Research* 44:4517-4528.
- 599 [36] Schmitt C, Vogt C, Van Ballaer B, Brix R, Suetens A, Schmitt-Jansen M, de Deckere
600 E. 2010. In situ cage experiments with *Potamopyrgus antipodarum*-A novel tool for real life
601 exposure assessment in freshwater ecosystems. *Ecotoxicology and Environmental Safety*
602 73:1574-1579.
- 603 [37] Matthiessen P. 2008. An assessment of endocrine disruption in Mollusks and the
604 potential for developing internationally standardized mollusk life cycle test guidelines.
605 *Integrated Environmental Assessment and Management* 4:274-284.
- 606 [38] Jacobsen R, Forbes VE, Skovgaard O. 1996. Genetic population structure of the
607 prosobranch snail *Potamopyrgus antipodarum* (Gray) in Denmark using PCR-RAPD
608 fingerprints. *Proceedings of the Royal Society B: Biological Sciences* 263:1065-1070.

- 609 [39] Mouthon J. 2001. Life cycle and population dynamics of the asian clam *Corbicula*
610 *fluminea* (Bivalvia: Corbiculidae) in the Rhône river at Creys-Malville (France). *Anglais* 151.
- 611 [40] Gust M, Buronfosse T, André C, Mons R, Gagné F, Garric J. 2011. Is exposure
612 temperature a confounding factor for the assessment of reproductive parameters of New
613 Zealand mudsnails *Potamopyrgus antipodarum* (Gray)? *Aquatic Toxicology* 101:396-404.
- 614 [41] Dorgelo J. 1987. Density fluctuations in populations (1982-1986) and biological
615 observations of *Potamopyrgus Jenkinsi* in two trophically differing lakes. *Hydrobiological*
616 *Bulletin* 21:95-110.
- 617 [42] Macken A, Le Page G, Hayfield A, Williams TD, Brown RJ. 2012. Effects of test
618 design and temperature in a partial life-cycle study with the freshwater gastropod
619 *Potamopyrgus antipodarum*. *Environmental Toxicology and Chemistry* 31:1989-1994.
- 620 [43] Winterbourn MJ. 1969. Water temperature as a factor limiting the distribution of
621 *Potamopyrgus antipodum* (Gastropoda Prosobranchia) in the New Zealand thermal region.
622 *New Zealand Journal of Marine and Freshwater Research* 3:453-458.
- 623 [44] Duft M, Schulte-Oehlmann U, Weltje L, Tillmann M, Oehlmann J. 2003. Stimulated
624 embryo production as a parameter of estrogenic exposure via sediments in the freshwater
625 mudsnail *Potamopyrgus antipodarum*. *Aquatic Toxicology* 64:437-449.
- 626 [45] Lefkovitch LP. 1965. The study of population growth in organisms grouped by stages.
627 *Biometrics* 21:1-18.

- 628 [46] Caswell H, Shyu E. 2012. Sensitivity analysis of periodic matrix population models.
629 *Theoretical Population Biology* 82:329-339.
- 630 [47] Caswell H, Trevisan MC. 1994. Sensitivity analysis of periodic matrix models.
631 *Ecology* 75:1299-1303.
- 632 [48] Chaumot A, Charles S, Flammarion P, Garric J, Auger P. 2002. Using aggregation
633 methods to assess toxicant effects on population dynamics in spatial systems. *Ecological*
634 *Applications* 12:1771-1784.
- 635 [49] R Development Core Team. 2008. R: A Language and Environment for Statistical
636 Computing. R Foundation for Statistical Computing.
- 637 [50] Kerans BL, Dybdahl MF, Gangloff MM, Jannot JE. 2005. Potamopyrgus
638 antipodarum: Distribution, density, and effects on native macroinvertebrate assemblages in
639 the Greater Yellowstone Ecosystem. *Journal of the North American Benthological Society*
640 24:123-138.
- 641 [51] Schreiber ESG, Glaister A, Quinn GP, Lake PS. 1998. Life history and population
642 dynamics of the exotic snail Potamopyrgus antipodarum (Prosobranchia: Hydrobiidae) in
643 Lake Purrumbete, Victoria, Australia. *Marine and Freshwater Research* 49:73-78.
- 644 [52] Richards DC, Shinn DC. 2004. Intraspecific competition and development of size
645 structure in the invasive snail Potamopyrgus antipodarum (Gray, 1853). *American*
646 *Malacological Bulletin* 19:33-37.

- 647 [53] Quinn GP, Lake PS, Schreiber ESG. 1996. Littoral benthos of a Victorian lake and its
648 outlet stream: Spatial and temporal variation. *Austral Ecology* 21:292-301.
- 649 [54] Dahl A, Winther LB. 1993. Life-history and growth of the prosobranch snail
650 *Potamopyrgus jenkinsi* in Lake Esrom, Denmark. *Verh Internat Verein Limnol* 25:582-586.
- 651 [55] Sternberg RM, Gooding MP, Hotchkiss AK, LeBlanc GA. 2010. Environmental-
652 endocrine control of reproductive maturation in gastropods: Implications for the mechanism
653 of tributyltin-induced imposex in prosobranchs. *Ecotoxicology* 19:4-23.
- 654 [56] Ponder WF. 1988. *Potamopyrgus antipodarum* - A Molluscan coloniser of Europe and
655 Australia. *Journal of Molluscan Studies* 54:271-285.
- 656 [57] Moller V, Forbes VE, Depledge MH. 1994. Influence of acclimation and exposure
657 temperature on the acute toxicity of cadmium to the freshwater snail *Potamopyrgus*
658 *antipodarum* (hydrobiidae). *Environmental Toxicology and Chemistry* 13:1519-1524.
- 659 [58] Wallace C. 1979. Notes on the occurrence of males in populations of *Potamopyrgus*
660 *jenkensi*. *Journal of Molluscan Studies* 45:61-67.
- 661 [59] Baird DJ, Brown SS, Lagadic L, Liess M, Maltby L, Moreira-Santos M, Schulz R,
662 Scott GI. 2007. In situ-based effects measures: determining the ecological relevance of
663 measured responses. *Integrated environmental assessment and management* 3:259-267.

664 [60] Liber K, Goodfellow W, den Besten P, Clements W, Galloway T, Gerhardt A, Green
665 A, Simpson S. 2007. In situ-based effects measures: considerations for improving methods
666 and approaches. *Integrated environmental assessment and management* 3:246-258.

667 [61] Gust M, Buronfosse T, Geffard O, Coquery M, Mons R, Abbaci K, Giamberini L,
668 Garric J. 2011. Comprehensive biological effects of a complex field poly-metallic pollution
669 gradient on the New Zealand mudsnail *Potamopyrgus antipodarum* (Gray). *Aquatic*
670 *Toxicology* 101:100-108.

671 [62] Jensen A, Forbes VE, Parker Jr ED. 2001. Variation in cadmium uptake, feeding rate,
672 and life-history effects in the gastropod *Potamopyrgus antipodarum*: Linking toxicant effects
673 on individuals to the population level. *Environmental Toxicology and Chemistry* 20:2503-
674 2513.

675 [63] Biro PA, Post JR. 2008. Rapid depletion of genotypes with fast growth and bold
676 personality traits from harvested fish populations. *Proceedings of the National Academy of*
677 *Sciences of the United States of America* 105:2919-2922.

678 [64] Jørgensen C, Enberg K, Dunlop ES, Arlinghaus R, Boukal DS, Brander K, Ernande B,
679 Gårdmark A, Johnston F, Matsumura S, Pardoe H, Raab K, Silva A, Vainikka A, Dieckmann
680 U, Heino M, Rijnsdorp AD. 2007. Ecology: Managing evolving fish stocks. *Science*
681 318:1247-1248.

682

683

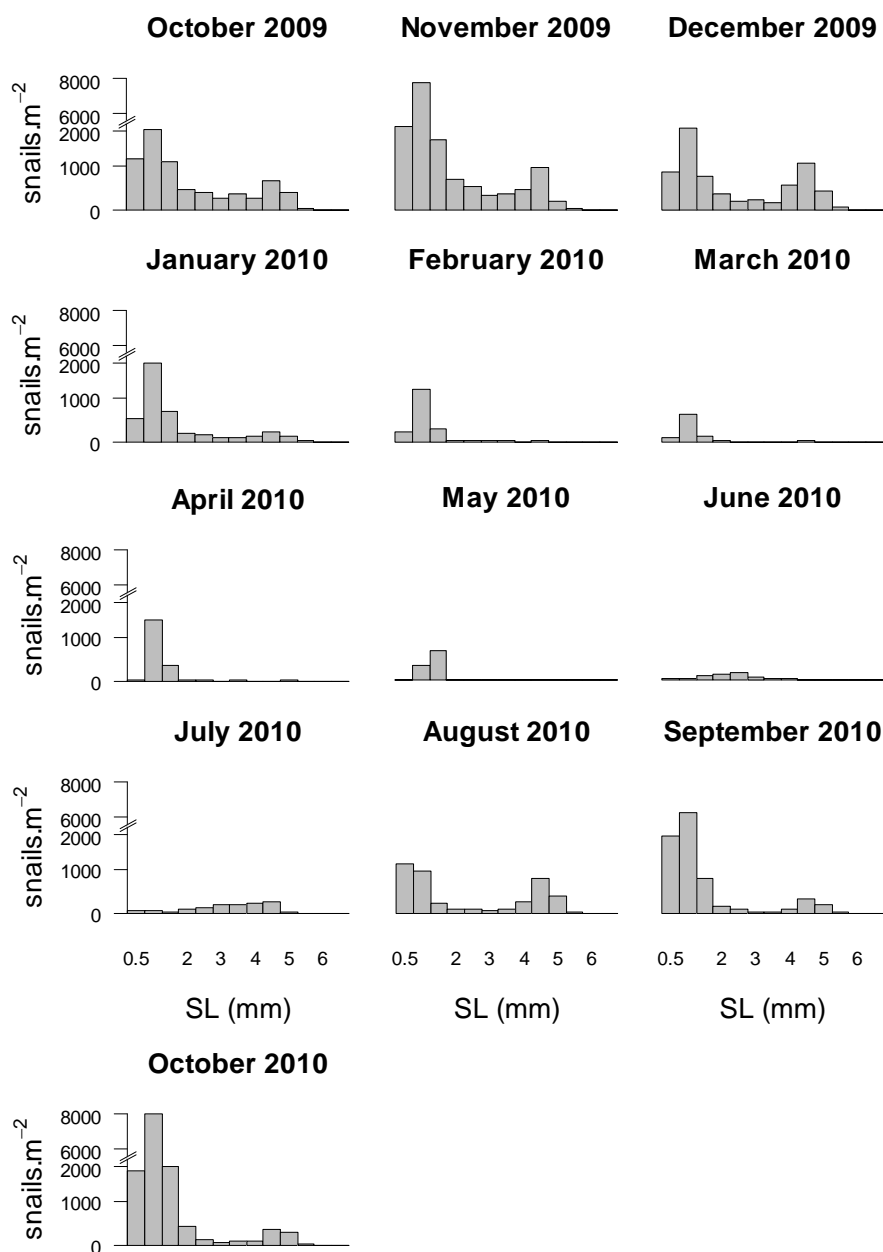


Figure 1.

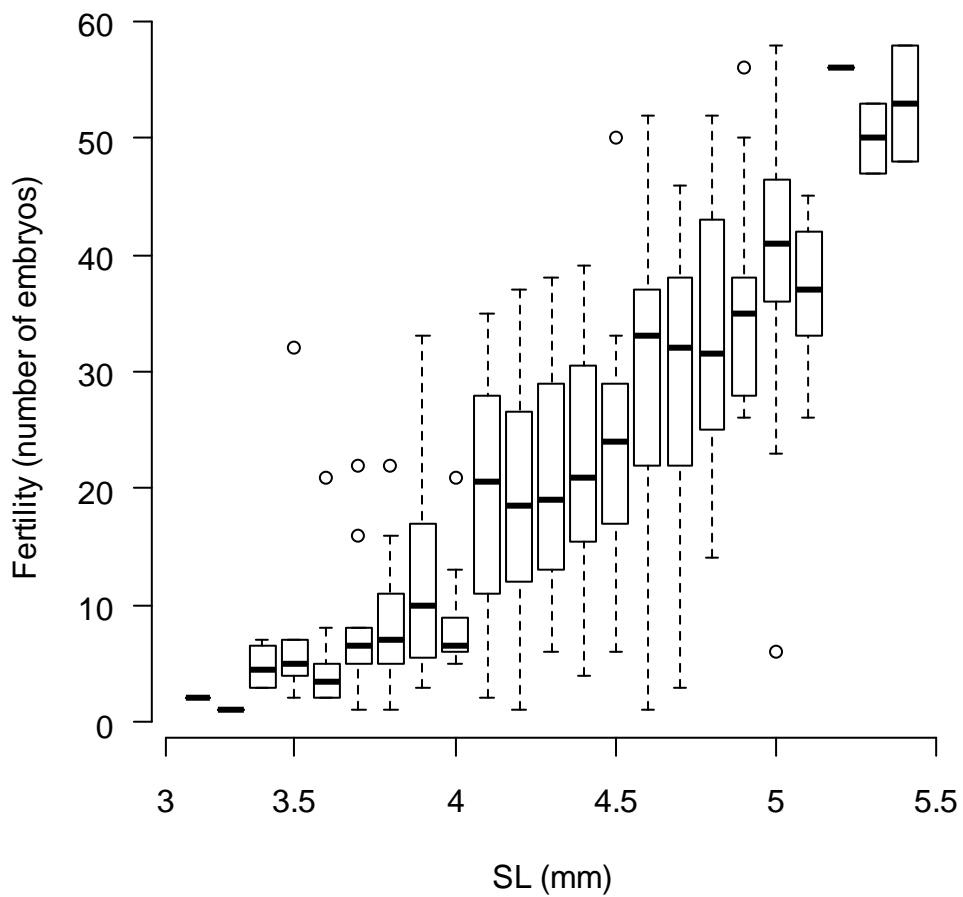


Figure 2.

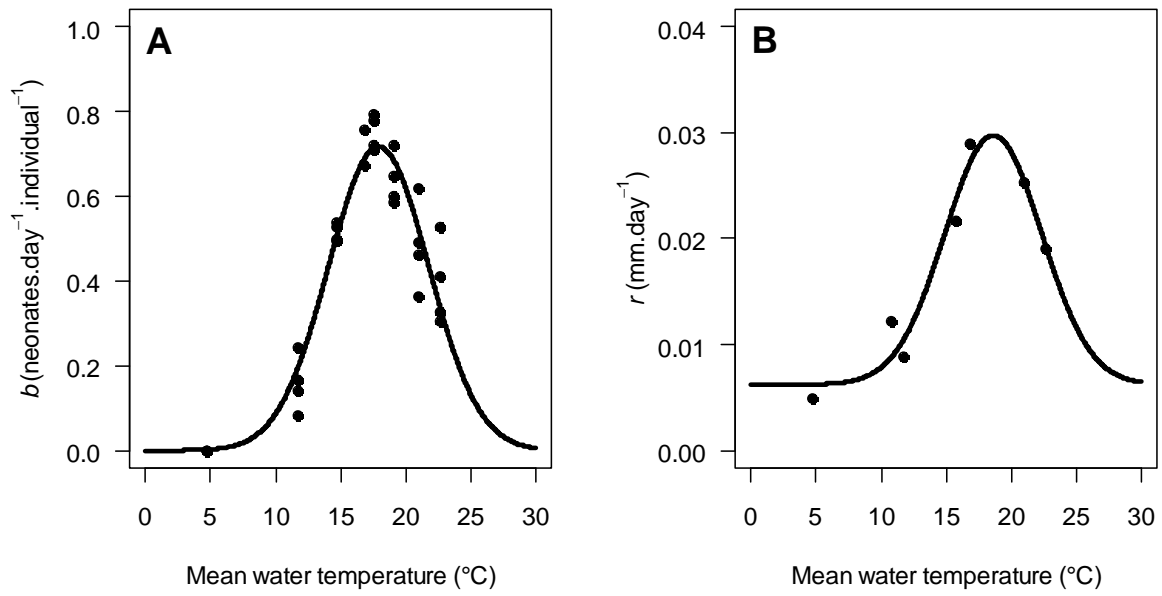


Figure 3.

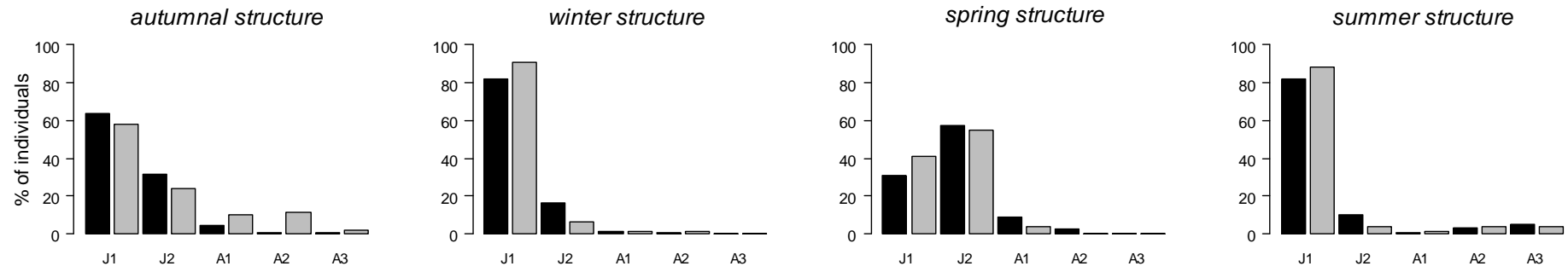


Figure 4.

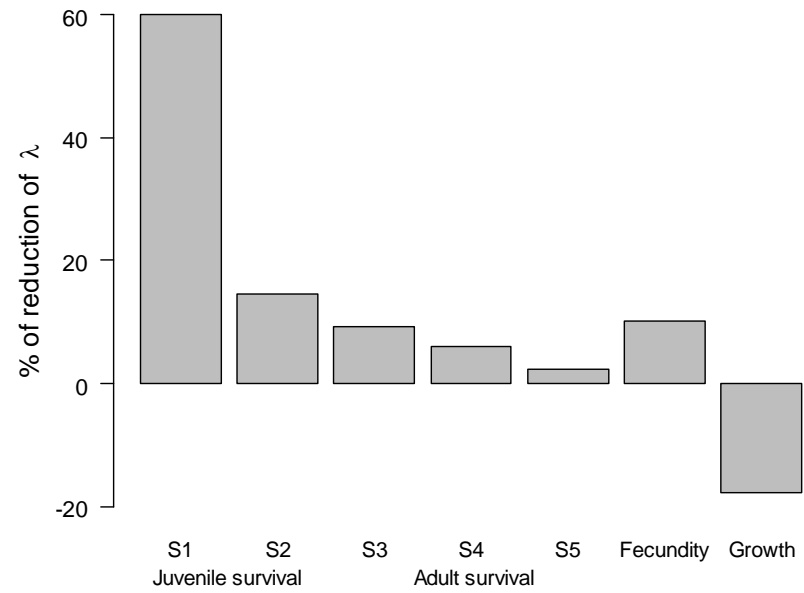


Figure 5.

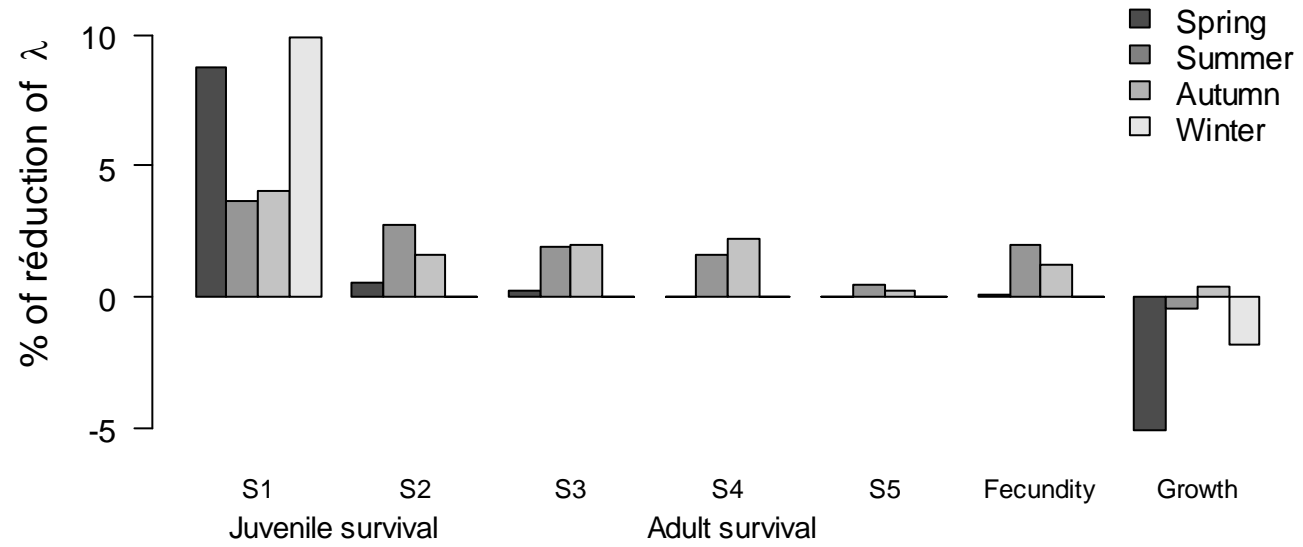
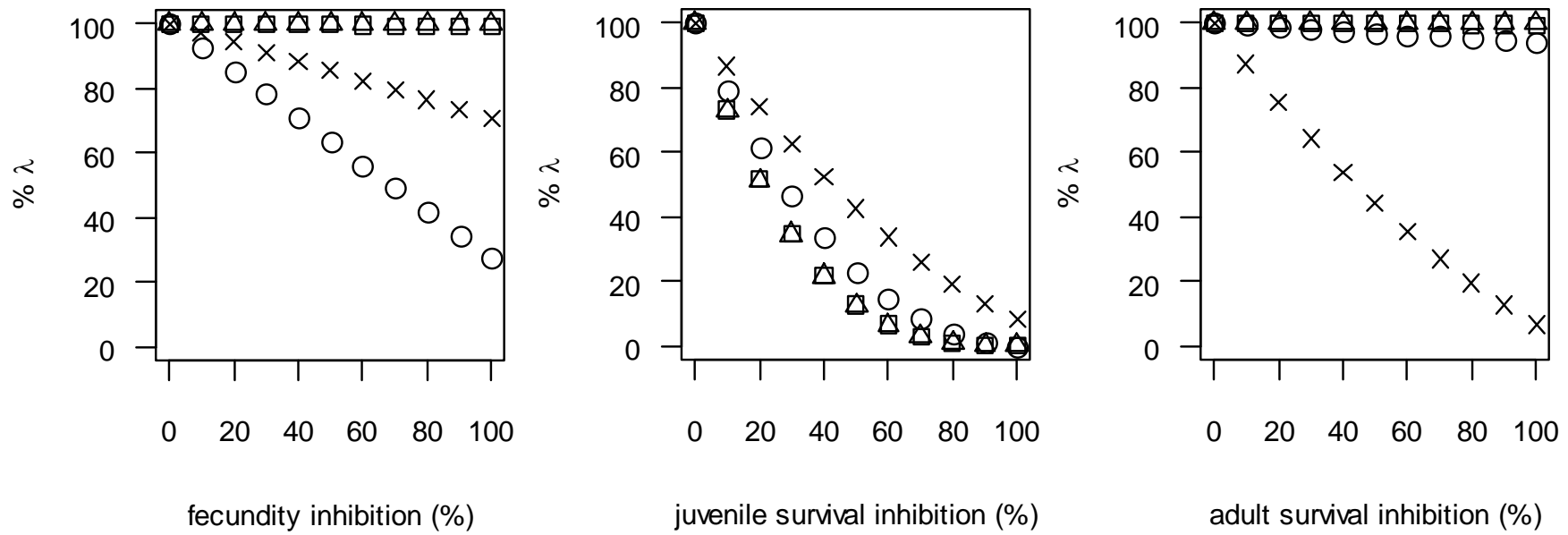


Figure 6.



1

2

3

4 **Figure 7.**